X-622-67-445

NASA TM X-55918

PRELIMINARY RESULTS FROM AN AIRCRAFT-BORNE MEDIUM RESOLUTION RADIOMETER

B.A. SPARKMAN

G.T. CHERRIX

M.S. TOBIN

SEPTEMBER 1967

GODDARD SPACE FLIGHT CENTER

GREENBELT, MARYLAND

X-622-67-445

PRELIMINARY RESULTS FROM AN AIRCRAFT-BORNE MEDIUM RESOLUTION RADIOMETER

B. A. Sparkman
G. T. Cherrix
M. S. Tobin

September 1967

GODDARD SPACE FLIGHT CENTER
Greenbelt, Maryland

PRECEDING PAGE BLANK NOT FILMED.

CONTENTS

ILLUSTRATIONS (Continued)

ILLUSTRATIONS

ILLUSTRATIONS (Continued)

ABSTRACT

A series of fourteen flights of the NASA Convair 990 research aircraft carrying a number of meteorologically-oriented instruments was carried out during May and June 1967. One of these instruments was a five-channel, medium resolution, scanning radiometer.

Surface temperature plots of data from the 10-to-11 micron channel of the radiometer over areas of Southern California showing differences in temperatures of lava, deserts, and salt beds in the same area are presented. These temperatures measured at different altitudes also show the large effect haze layers have on 10-to-11 micron measurements.

An increase in the spectral reflectance of an ocean surface caused by the kelp beds off the coast of San Diego is shown.

Bidirectional reflectances of stratocumulus clouds and ocean surfaces were measured with the 0.2 to 4 micron channel of the radiometer. These measurements were made in four azimuthal directions with respect to the principal plane of the sun. Values of bidirectional reflectances obtained agree well with those obtained during a series of flights of the same radiometer on the NASA Convair 990 in 1966.

PRELIMINARY RESULTS FROM AN AIRCRAFT BORNE MEDIUM RESOLUTION RADIOMETER

I. INTRODUCTION

During the spring of 1967 radiometric observations in the infrared and visible spectral regions of various geographical surfaces were made with a Medium Resolution Infrared Radiometer, (MRIR), flown aboard NASA's Convair-990 research aircraft.

These measurements were made to help define bidirectional reflectances from various surfaces of meteorological interest, to construct thermal graphs of various earth surfaces for comparison with similar measurements from satellites, and to provide apparent surface temperatures as support data for a microwave radiometer which was flown concurrently.

In this preliminary report we present: thermal plots showing temperature and reflectance changes over lava, deserts, and saltflats of southern California; bidirectional reflectances from cloud and ocean surfaces; and some measurements showing the influence of the kelp beds off the coast of San Diego on ocean surface reflectances.

II. DESCRIPTION OF THE RADIOMETER

The Airborne Medium Resolution Infrared Radiometer (MRIR) is an early Flight model (F-3) of the Nimbus type, 5 channel Medium Resolution Infrared Radiometer.* Three of the channels (See Figure 1) respond to radiation in the infrared region of the spectrum, (Channel 1, at 6.7μ, 2 at 10μ to 11μ, and 4 at 5μ to 30μ). Channels 3 (0.55μ to 0.85μ) and 5 (0.2μ to 4μ) respond to short wave radiation.

Figure 2 shows the MRIR without modifications for mounting on the aircraft. Figure 3 is a diagram of the optical system of each channel. Only the filter (F)

*The term "Medium Resolution Infrared Radiometer" (MRIR) is actually a misnomer, since the satellite instrument contains a channel which responds in part to visible radiation (0.2μ to 4μ) and the airborne instrument contains two such channels (0.55μ to 0.85μ, and 0.2μ to 4μ). However, the term "MRIR" has been so widely adopted as to compel its use here.

**The Nimbus II User's Guide (July 1966), available from the Nimbus Project Office of the Goddard Space Flight Center, contains a complete description of this instrument. The basic MRIR is the same as the airborne MRIR.

is different for each channel. The scan mirror (M) is set at 45° to, and rotates about an axis parallel to the axes of the 5 cassegrainian telescopes such that each 50 by 50 milliradian field of view scans through a 360° arc in a plane perpendicular to the axis of rotation during its 7-1/2 second period. The airborne instrument scans in the vertical plane containing the longitudinal axis of the aircraft. The instrument was covered with a thick thermal foam jacket without obscuring the optics and scanning area. Heaters maintained the radiometer at 25°C. This assembly was shock mounted inside an aerodynamic fairing which was fastened to the underside of the aircraft's tail section. Figure 4 shows the MRIR in the aerodynamic fairing mounted on the Convair 990 jet aircraft. A motor operated door was provided in the fairing for protection of the optics during take-off and landing. Figure 5 represents the unobscured field of view of the five channels of the MRIR. Scanning is fore to aft in the downward viewing directions.

III. THERMAL PLOTS

Passes at 33,000, 10,000, and 3,000 feet were made over Bristol, Cadiz, and Danby dry lakes in Southern California. Figure 6 shows a plot of the aircraft track.

The readings at 0° nadir angle were taken from Ch 2 (10-11μ) and plotted against geographical position (Figure 7). Since the dry lakes have a higher reflectance and therefore absorb less solar energy than the surrounding areas, the Ch 2 surface temperature of the dry lakes, 309°K, is cooler than the desert and much cooler than the lava bed north of Bristol dry lake. There is very good agreement between the equivalent blackbody temperatures measured over all of the surfaces of Figure 7 from 33,000 and 10,000 feet. But the 3,000 foot altitude run shows a 9°K increase in equivalent blackbody temperature over the lava beds. This difference decreases to 3°K over Cadiz dry lake. These temperatures agree with those simultaneously measured with a filter wedge spectrometer in the 10-11 micron range, (Hovis, et al, 1967), and with measurements made from the Colorado State University Twin Comanche aircraft with a Barnes IT-2 radiometer, (Marlett, et al, 1967).

A radiosonde measurement from Vandenburg Air Force Base, shown in Figure 8, indicated a slight inversion below 10,000 feet.

From these data we may surmise that there is a thick haze layer below 10,000 feet over the lava beds and Bristol dry lake, and that this haze layer becomes thinner in the south toward Cadiz dry lake.

These data indicate that 10-11 micron surface temperature measurements made by satellites over desert areas can be as much as 9°K too cold.

The reflectance measurements (0.2 to 4μ) show some change with altitude as would be expected from atmospheric scattering in the visible. The 3,000 foot altitude data show much stronger reflectance variations between targets since there is less atmospheric interference at low altitudes. The dry lakes have a reflectance of about 30%.

IV. EFFECT OF KELP BEDS ON OCEAN SURFACE REFLECTANCE

A 1,000-foot pass was made over the "kelp beds" off the coast of San Diego. Downward looking photographs (Figures 9 and 10) showed a large difference in surface texture of the ocean when the kelp was present and when it was absent. Apparently the kelp smooths the surface and thus increases specular reflectance. Four cases of Ch 5 (0.2 to 4μ), measurements covering the range of nadir angles from 0° to 90° were investigated. Figure 11 shows a comparison between a normal sunlit ocean surface area and (a few seconds later) a sunlit kelp area. The peak specular reflectance is increased from 17% for the normal ocean surface to 40% for the kelp surface. The smoothing of the surface is also seen in the narrowing of the specular reflectance region when the kelp is present. Figure 12 shows the kelp's effect on reflectance with a cloud above. The peak reflectance is not changed since there is very little specular reflectance, but it is narrowed again due to smoothing of the surface. The peak reflectance is shifted from 19° to 27° probably because of multiple reflectances from the cloud surfaces above. The Ch 2 (10-11μ) surface temperature was unaffected by the kelp.

V. BIDIRECTIONAL REFLECTANCE MEASUREMENTS

Bidirectional reflectance measurements over clouds and open ocean were made to extend the range of solar zenith angles encompassed in similar measurements made during the 1966 flights. Due to limited flying time, the rosette pattern was reduced to a criss-cross type shown in Figure 13. With this pattern, only measurements in azimuthal directions of 0°, 90°, 180° and 270° can be obtained.

Figures 14 through 27 show bidirectional and directional reflectances for stratocumulus decks and ocean surfaces. The directional reflectance is obtained by integrating the bidirectional reflectances over the upward hemisphere.

Where the angular relationships overlapped, the results of these figures agree well with those obtained last year, with the total reflectance of the clouds being 28 to 47%. These data will be added to a catalog of bidirectional reflectances to be published in the near future.

CONCLUSIONS

These data indicate that the presents of haze can severely attenuate the upward stream of surface infrared radiation reducing the equivalent blackbody temperature measured in the 10-11 micron band. This effect occurred even when the haze layer was not readily apparent from downward looking photos. The haze layer was, however, noted by observers aboard the aircraft looking at it edge-on.

The specular reflectance of ocean surface is markedly greater over kelp beds than over ocean with no kelp beds.

Bidirectional reflectances of earth surfaces are strongly dependent on nadir, azimuth, and solar zenith angles. This effect should be accounted for when beam measurements from satellites are used to sum over the earth to obtain albedo.

REFERENCES

1. Private Communication from Dr. W. Hovis, Goddard Space Flight Center, Greenbelt, Maryland.

2. Private Communication from Dr. Marlatt, Colorado State University, Fort Collins, Colorado.

3. Cherrix, G. T. and B. A. Sparkman, "A Preliminary Report on Bidirectional Reflectances of Stratocumulus Clouds Measured With an Airborne Medium Resolution Radiometer," NASA-GSFC, X-622-67-48, (1967).

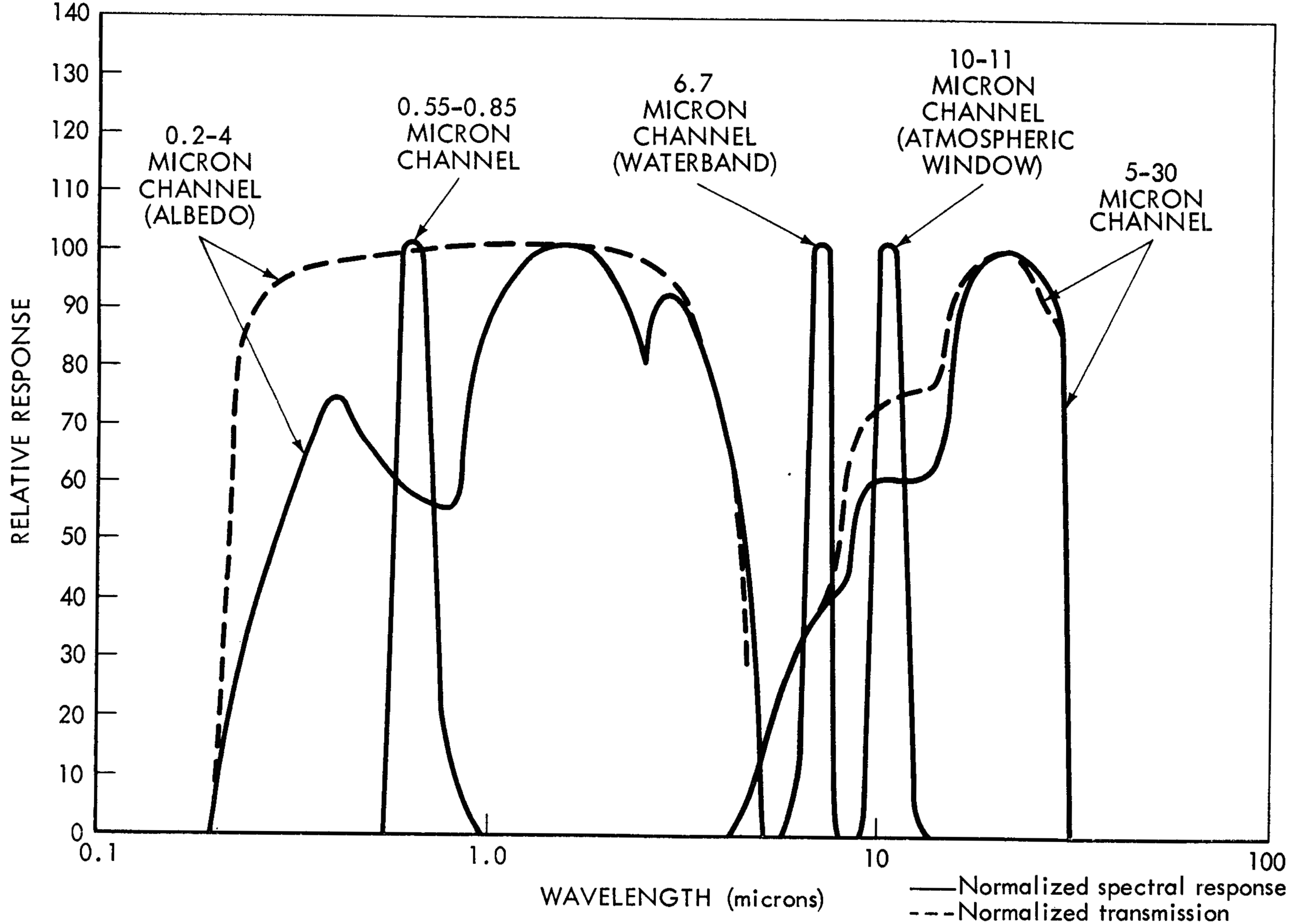

Figure 1. Filter and Relative Spectral Response of Nimbus Five-Channel Radiometer

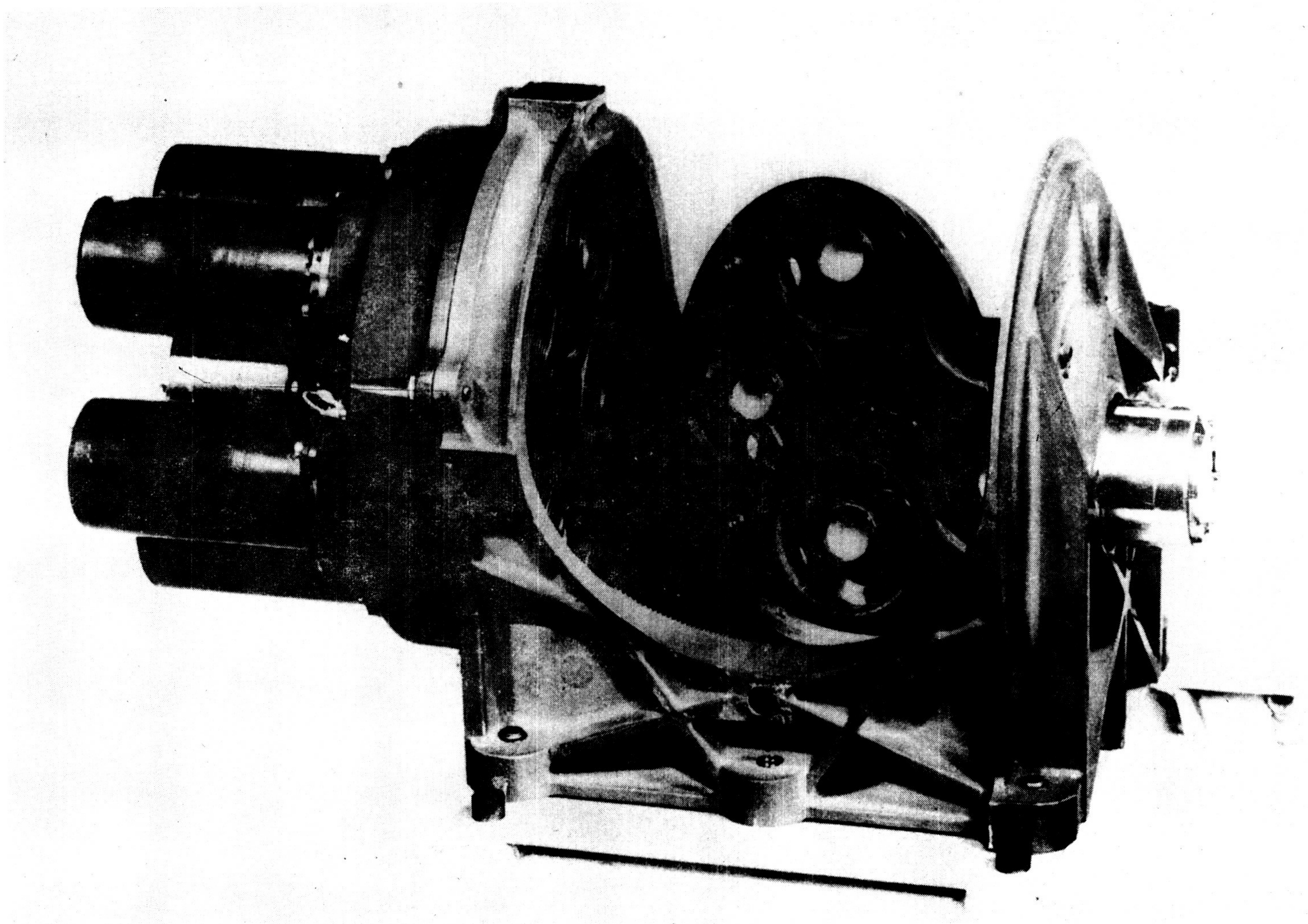

Figure 2. Medium Resolution Infrared Radiometer, (MRIR)

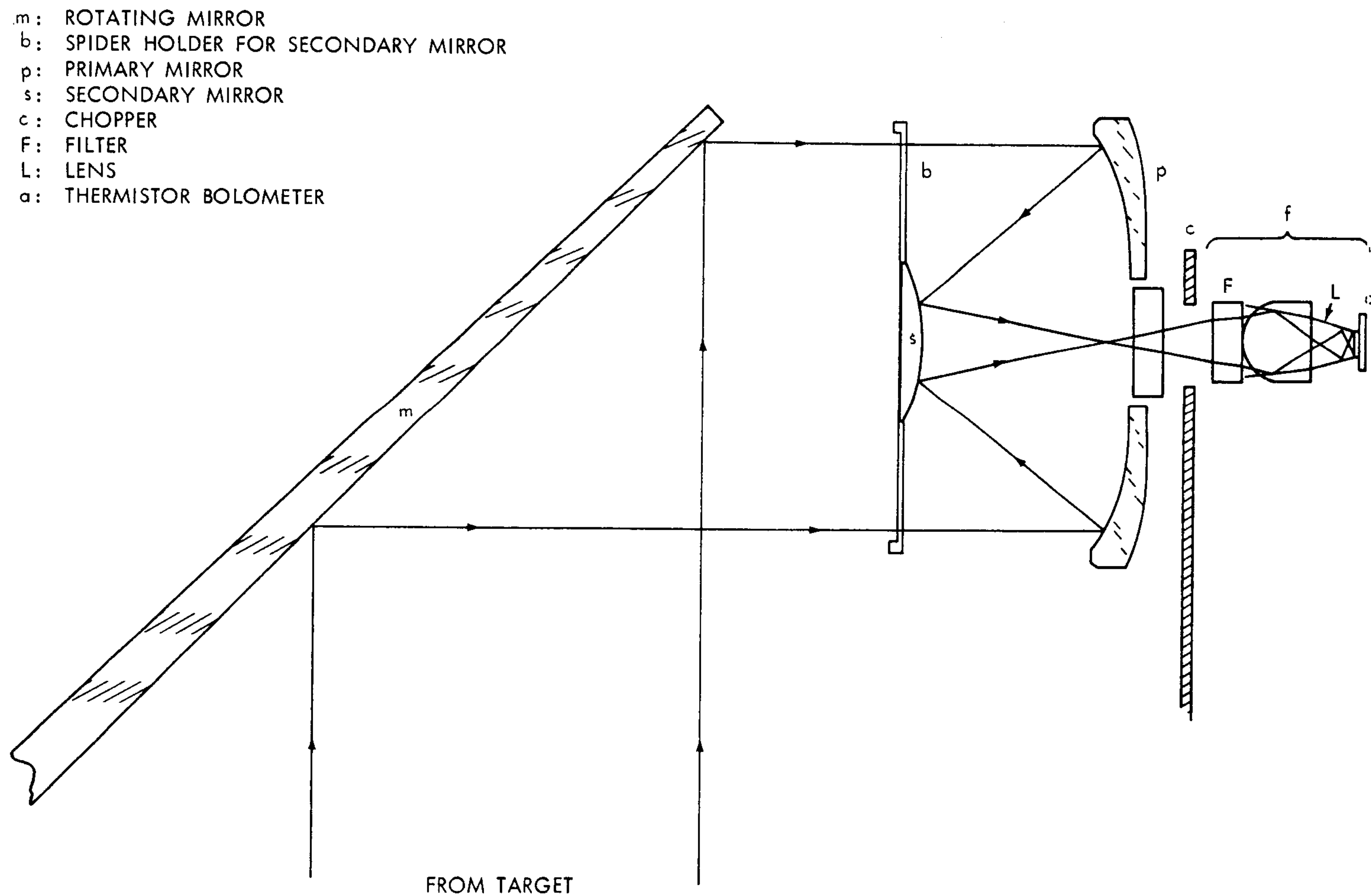

Figure 3. Optical System of the MRIR

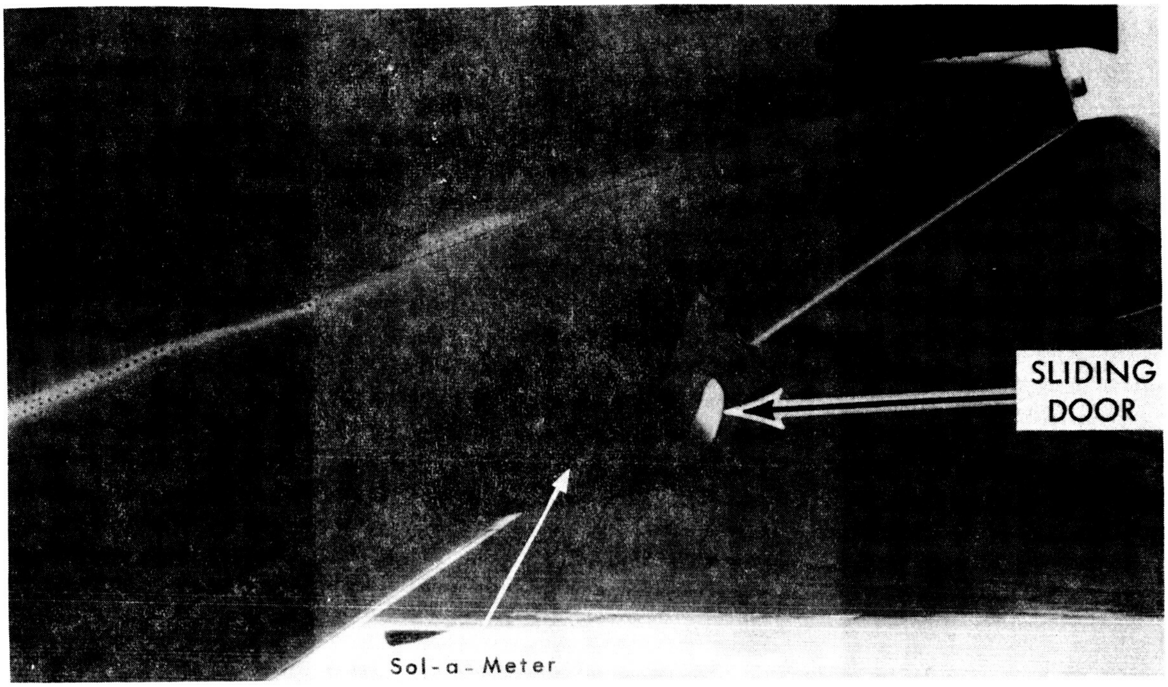

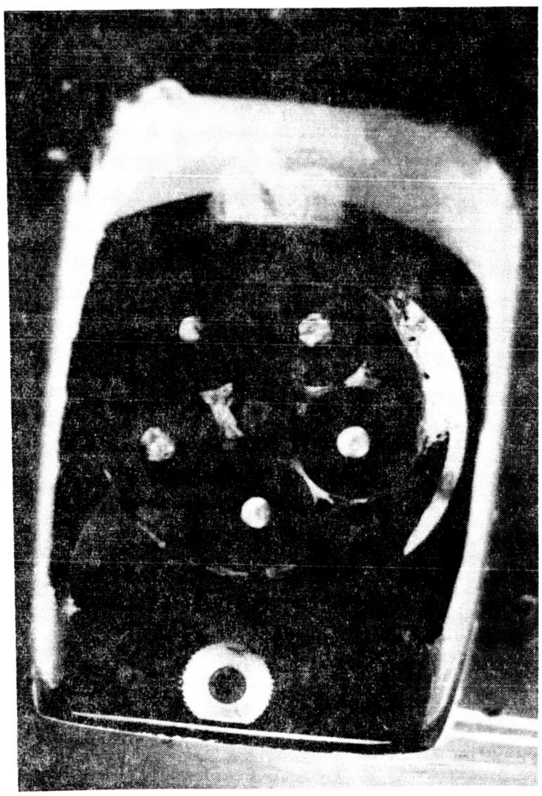

Figure 4. MRIR Mounted in Aircraft Fairing

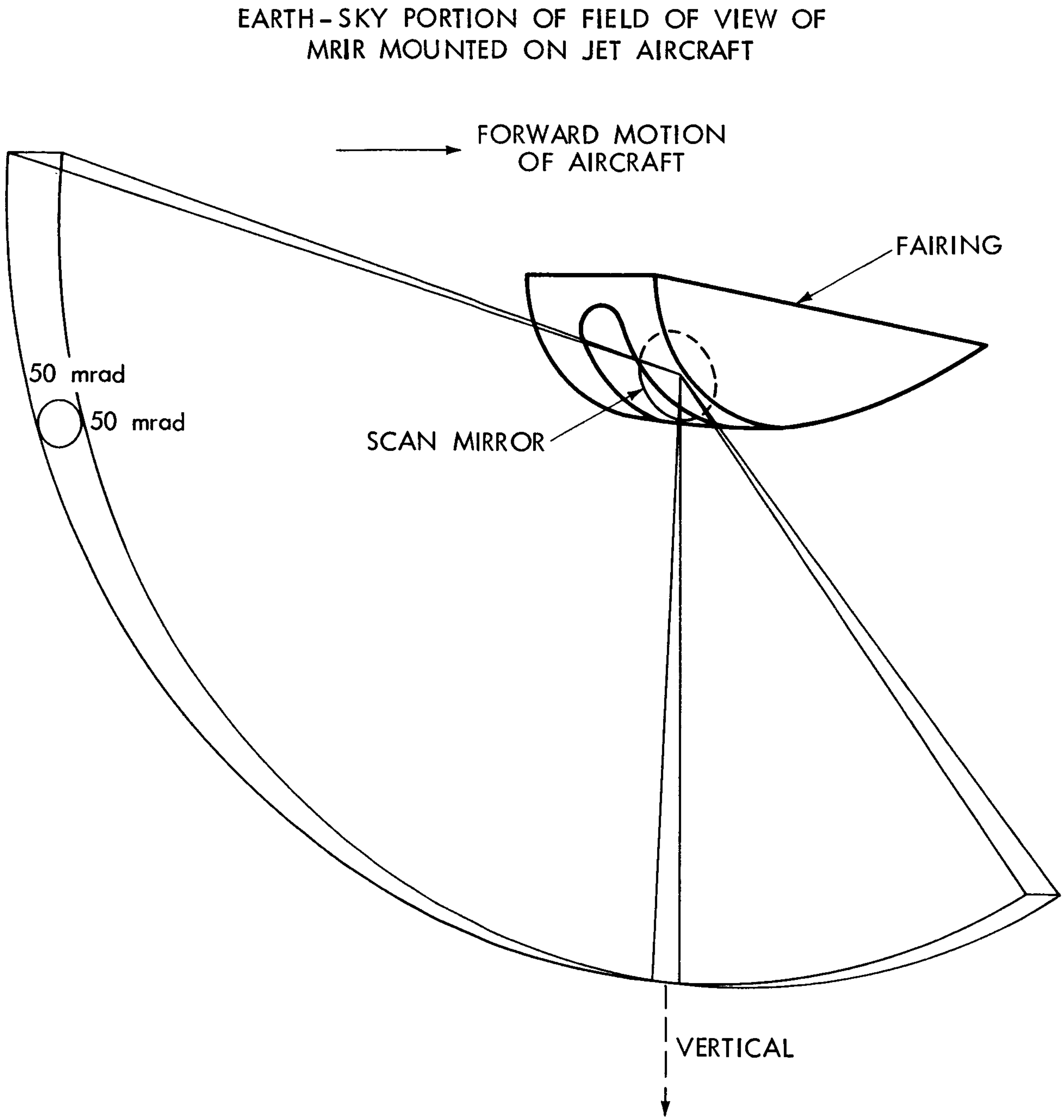

Figure 5. Earth-Sky Portion of View of MRIR Mounted on Jet Aircraft

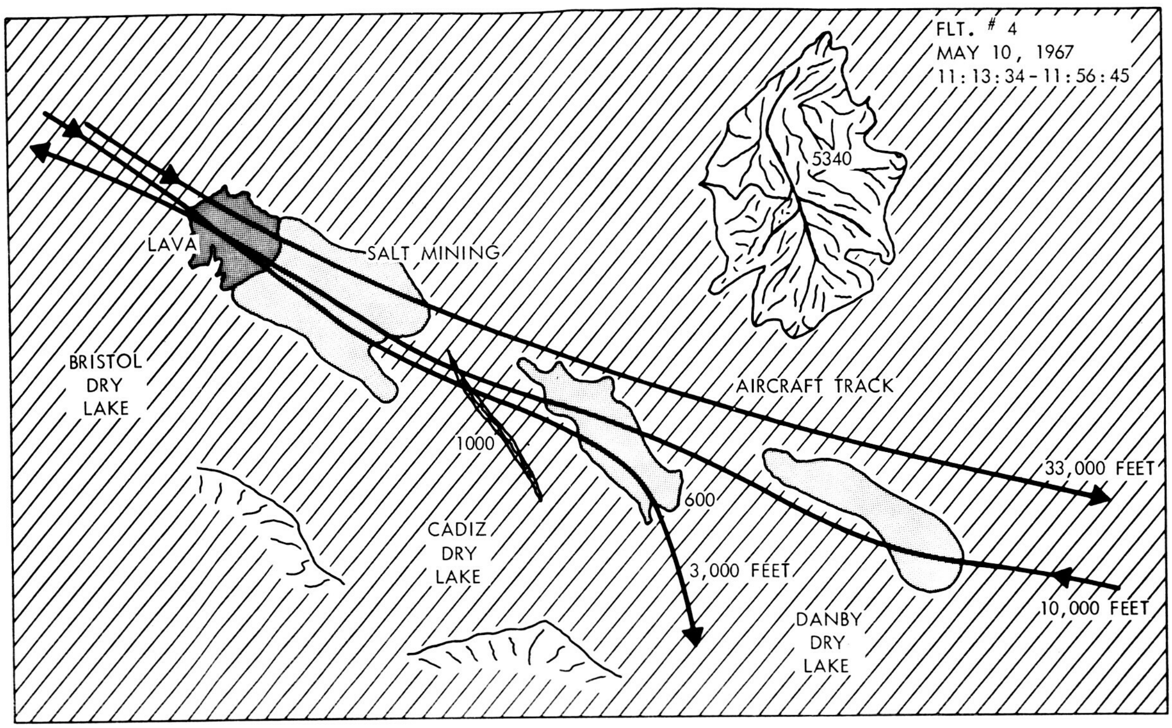

Figure 6. Area Map Showing Flight Path

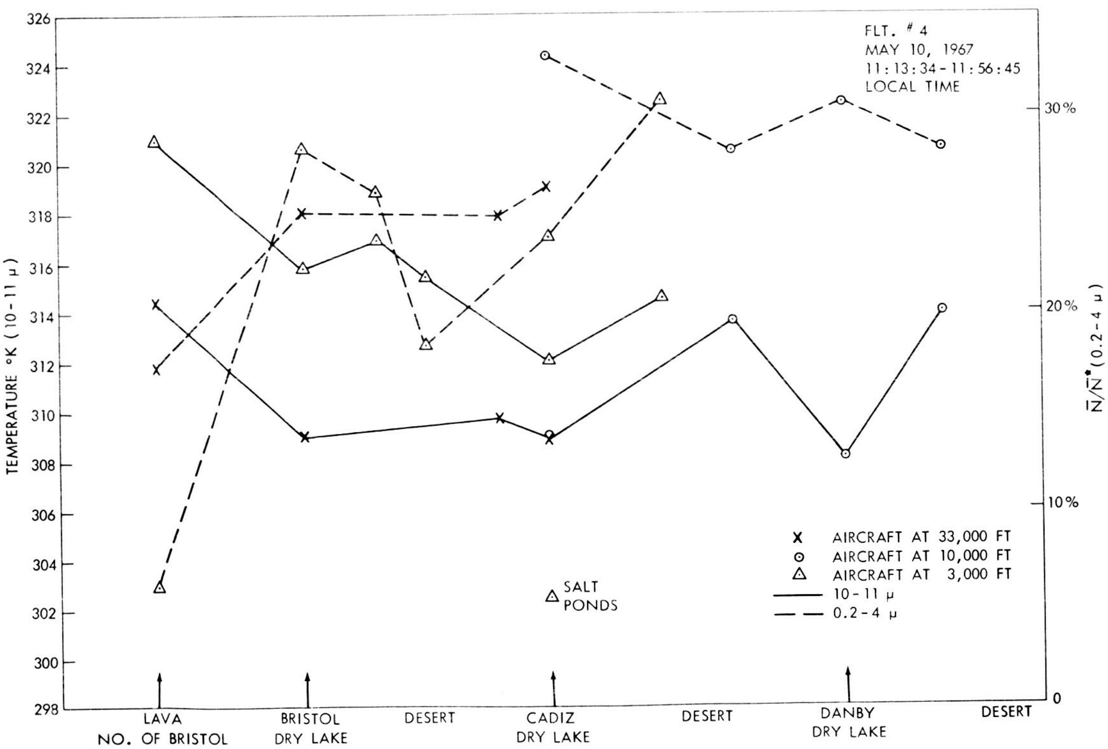

Figure 7. Surface Temperature and Reflectance Across Dry Lakes

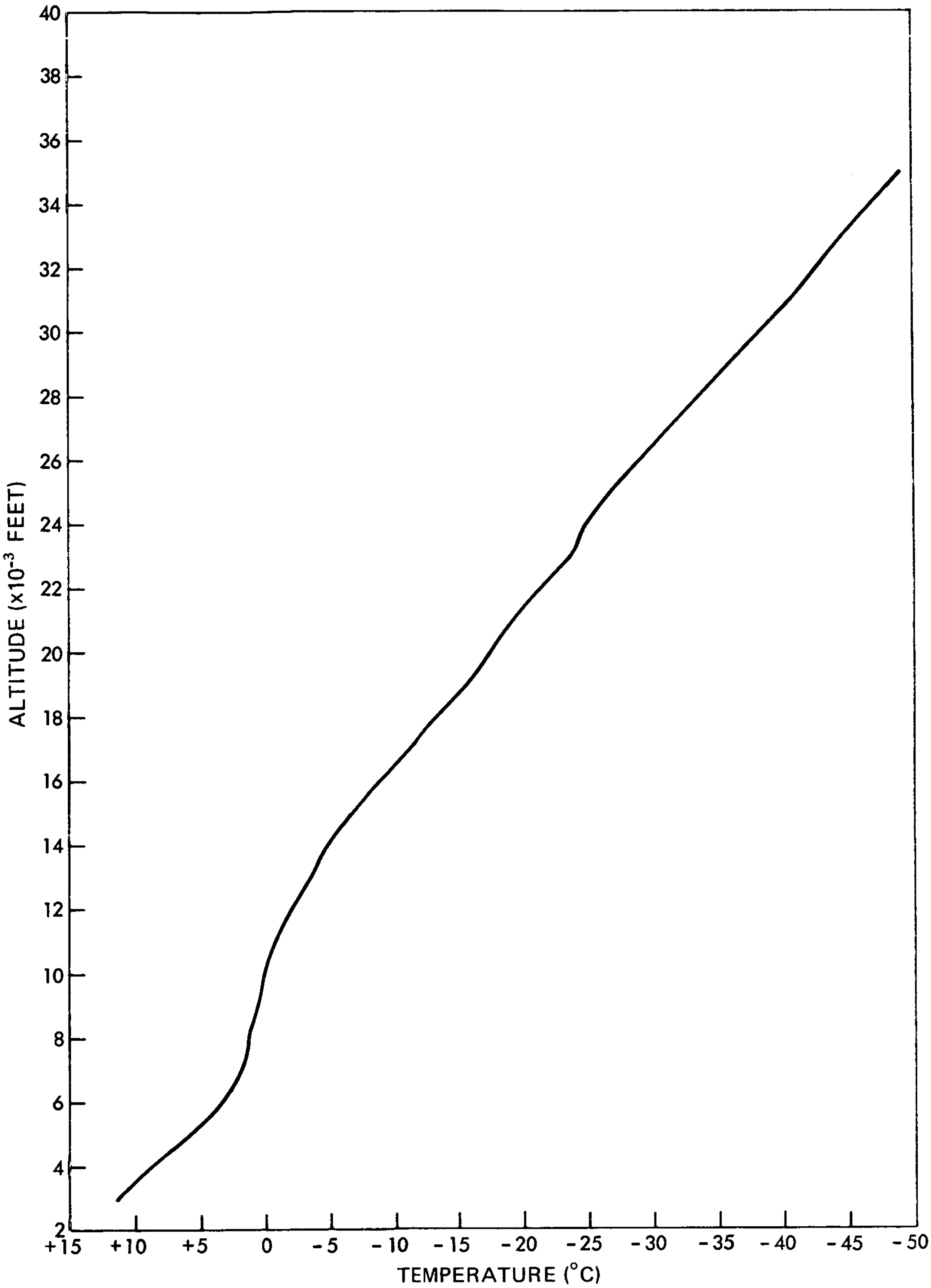

Figure 8. Air Temperatures From Radiosonde Measurements at Vandenburg Air Force Base

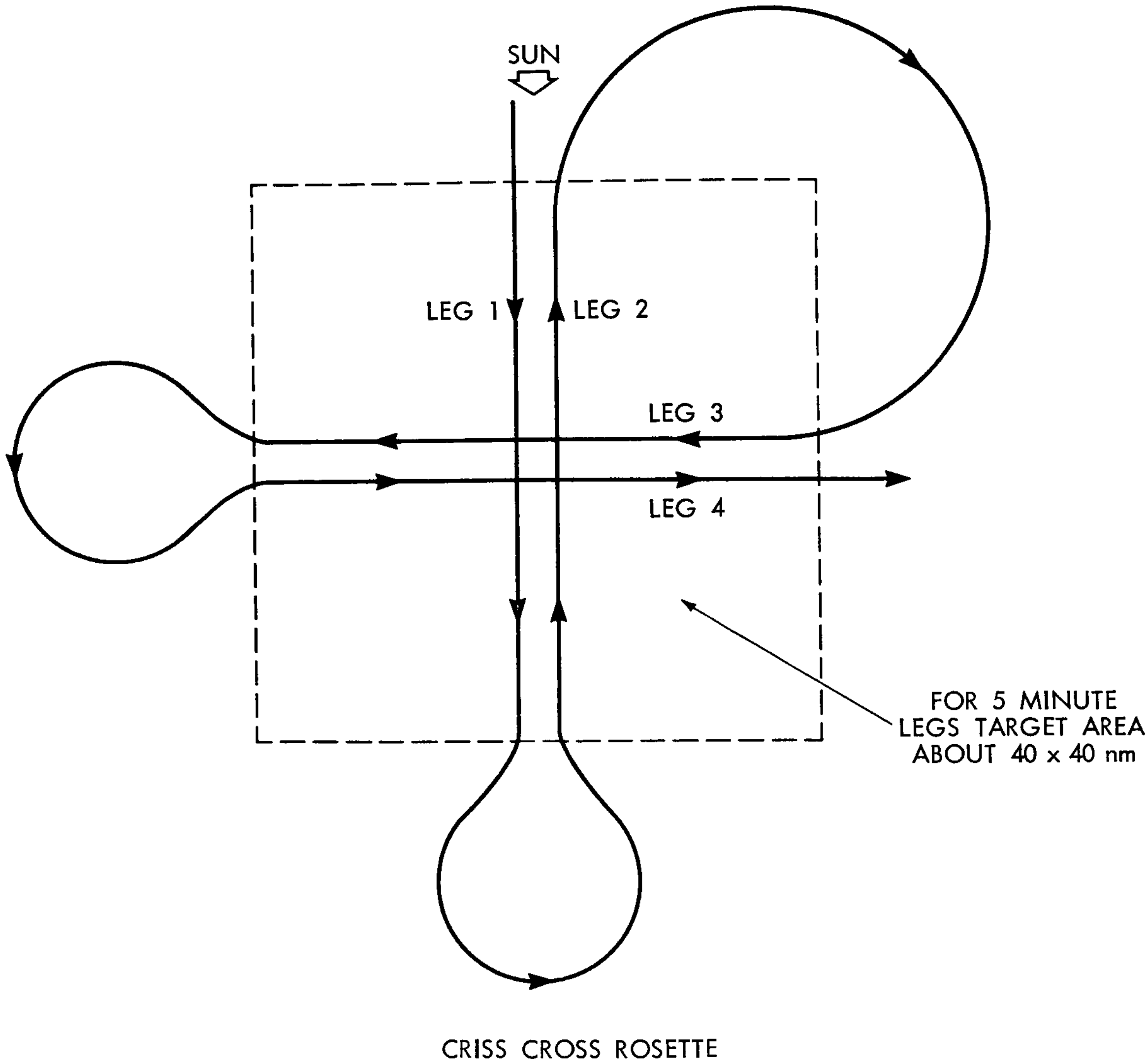

Figure 9. Criss Cross Rosette

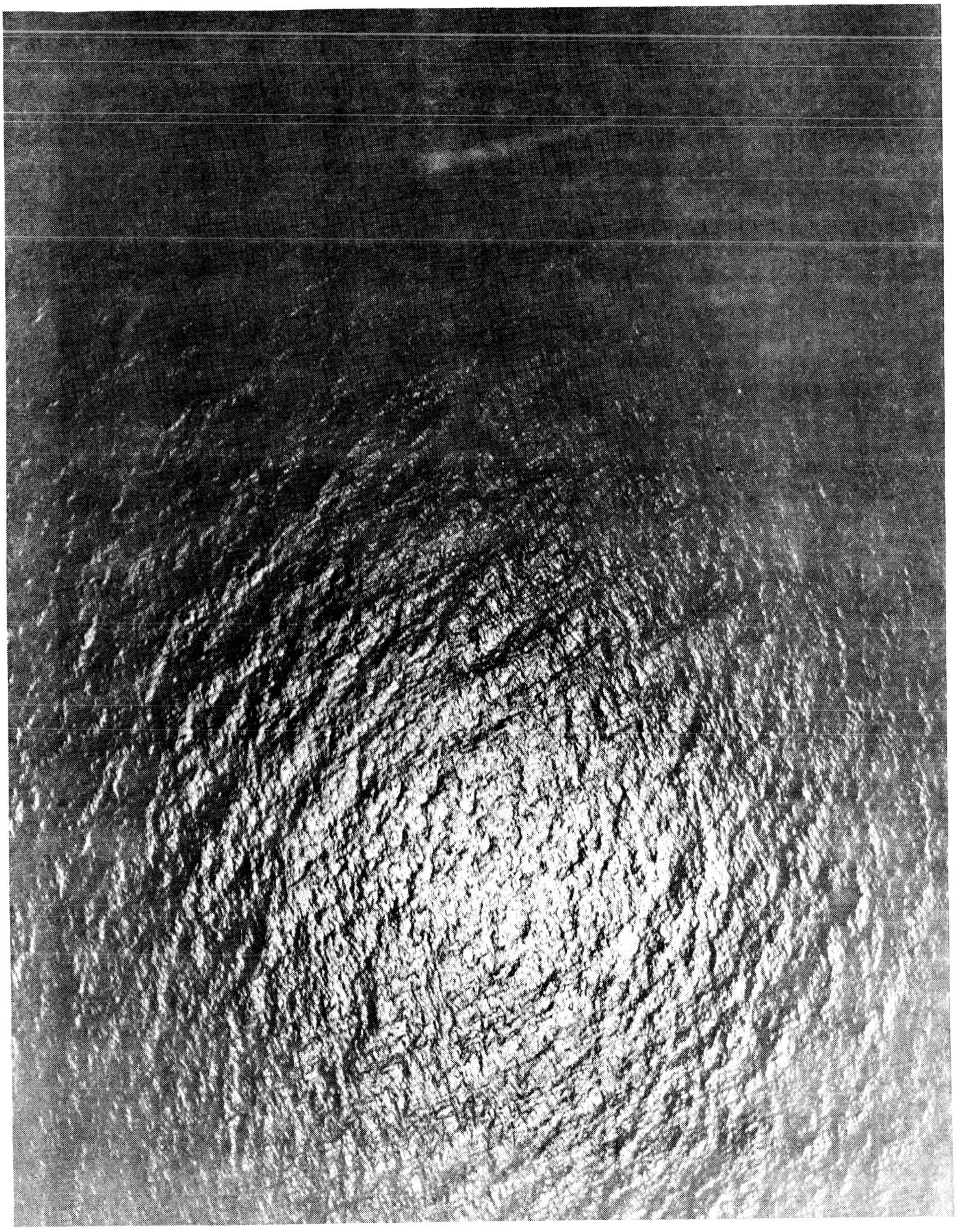

Figure 10. Normal Ocean Surface Texture

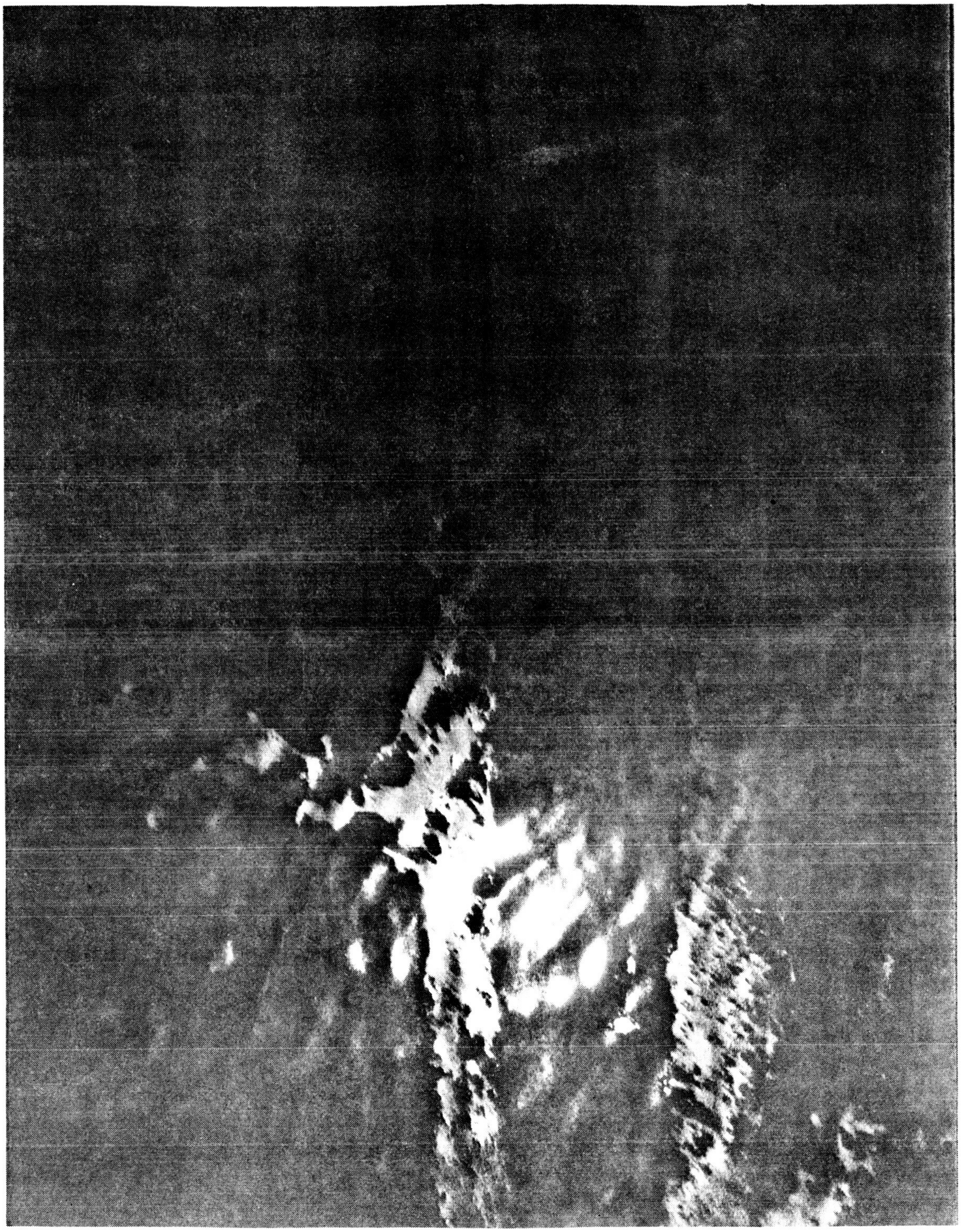

Figure 11. Kelp Bed Smoothing Ocean Surface Texture

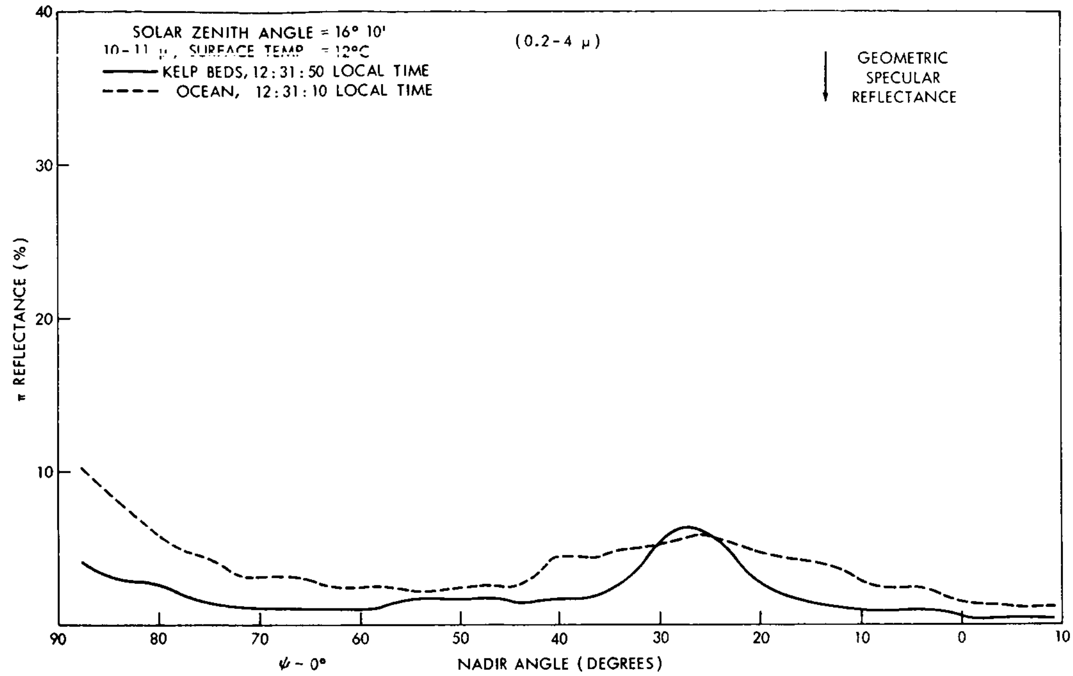

Figure 12. Effect of Kelp Beds on Ocean Surface Reflectance with Cloud Above

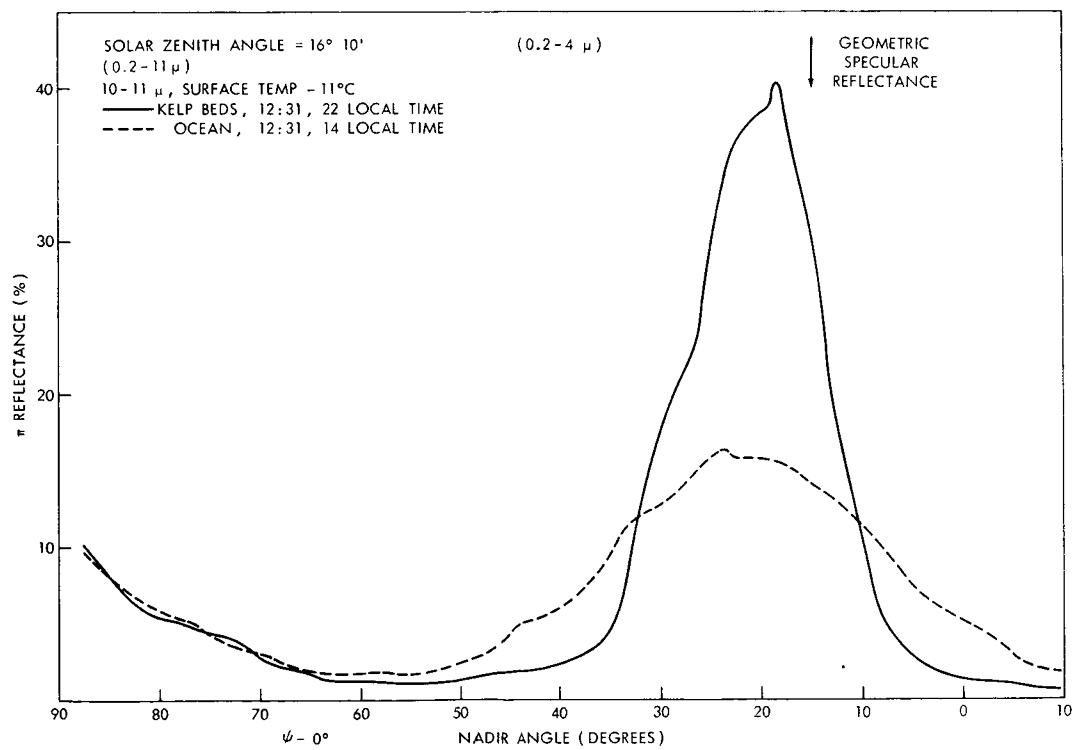

Figure 13. Effect of Kelp Beds on Ocean Surface Reflectance in Sunlight

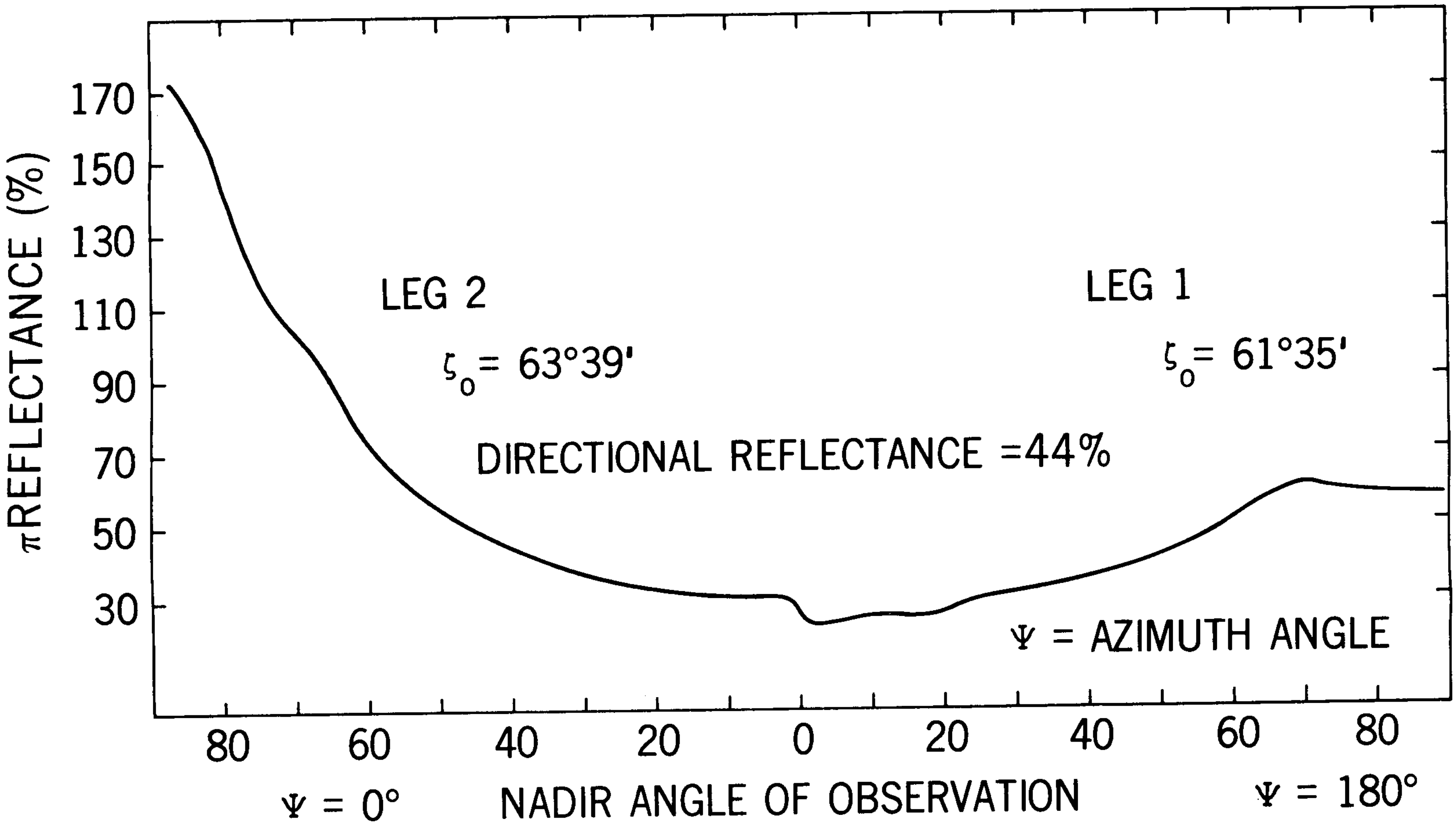

Figure 14. NASA Convair 990 Flight 1, May 6, 1967 (Altitude 25,000 feet) Uniform Stratocumulus (Altitude ~4,500 feet) 34°N 122°W (0031 UT to 0107 UT) MRIR Channel 5 (0.2 to 4μ)

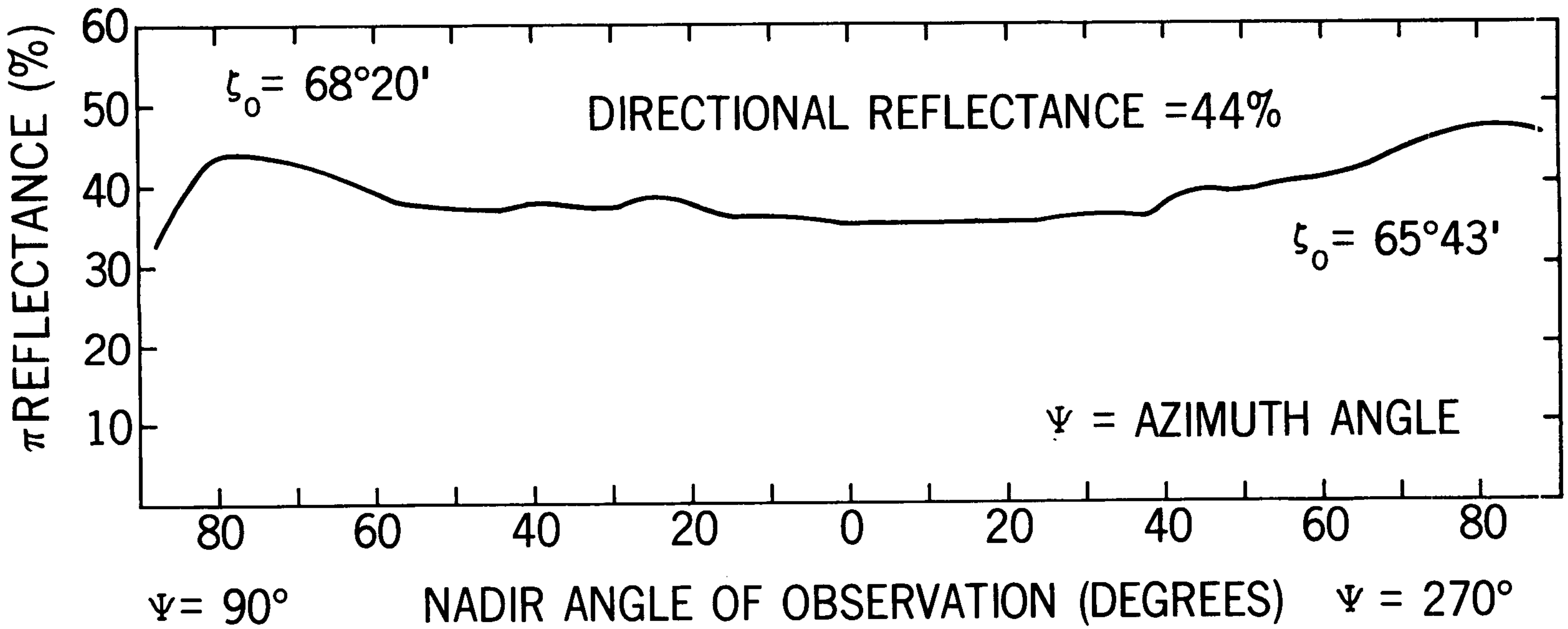

Figure 15. NASA Convair 990 Flight 1, May 6, 1967 (Altitude 25,000 feet) Uniform Stratocumulus (Altitude ~ 4,500 feet) 34°N 122°W (0031 UT to 0107 UT) MRIR Channel 5 (0.2 to 4μ)

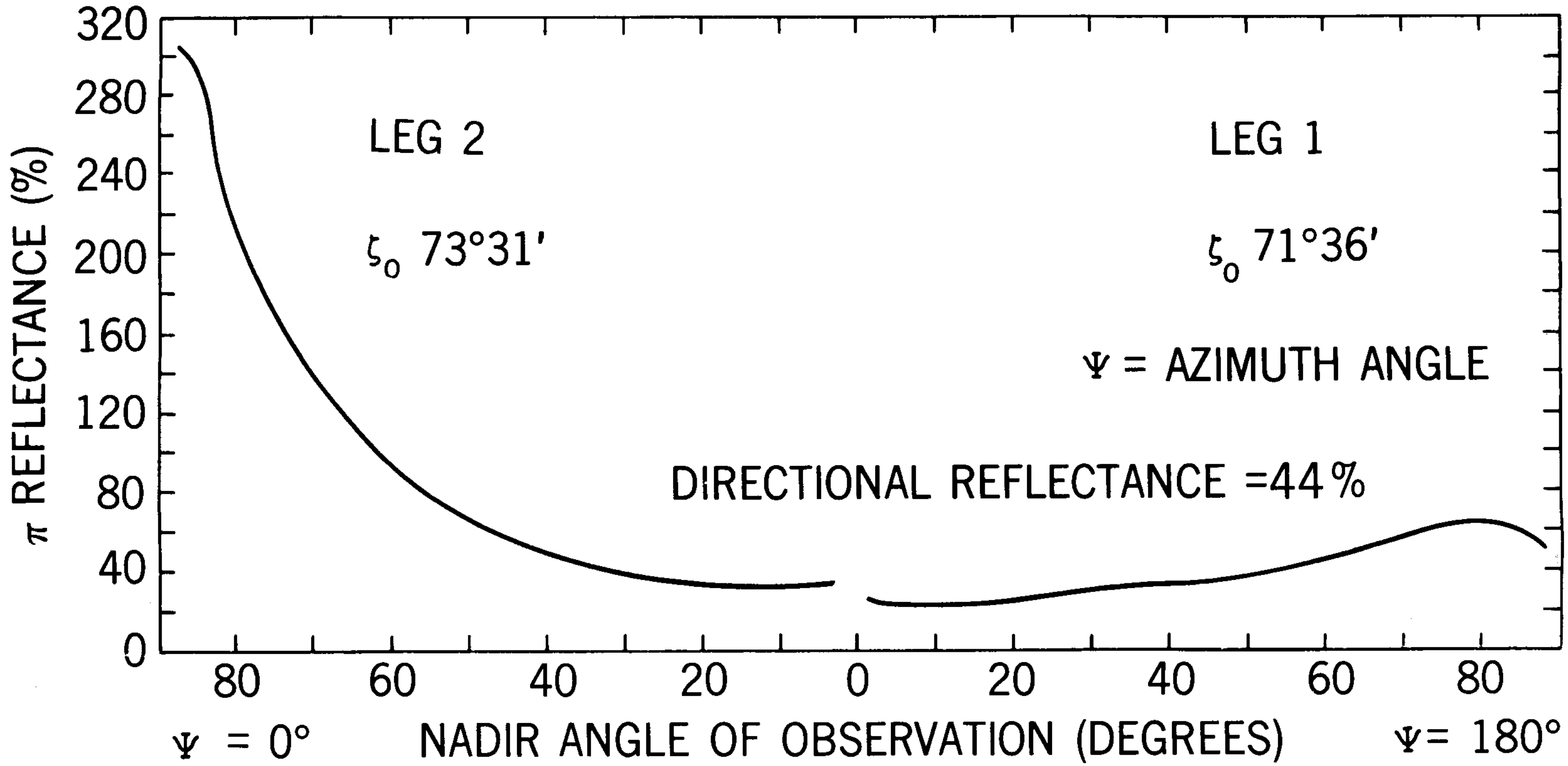

Figure 16. NASA Convair 990 Flight 1, May 6, 1967 (Altitude 35,300 feet) Uniform Stratocumulus Deck (Altitude ~ 4,500 feet) 34° 07'N 122°30'W (0119 UT to 0200 UT)

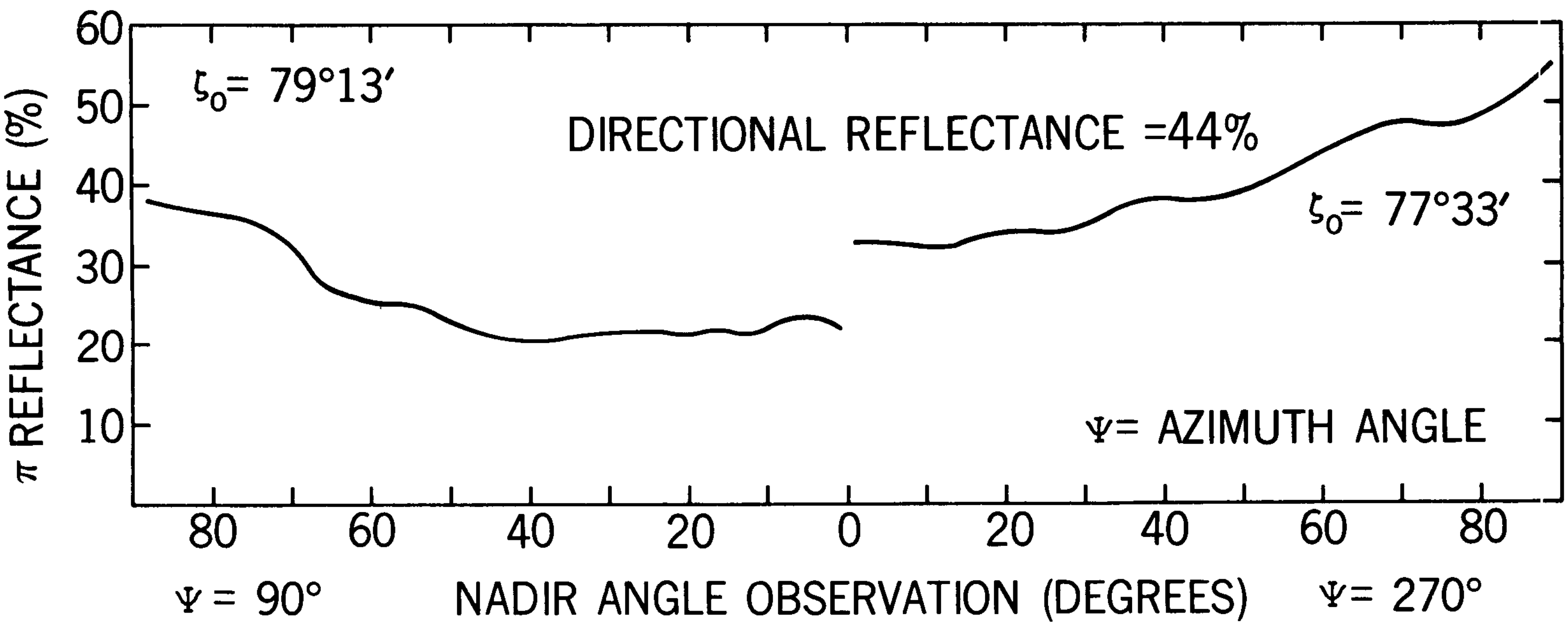

Figure 17. NASA Convair 990 Flight 1, May 6, 1967 (Altitude 35,300 feet) Uniform Stratocumulus Deck (Altitude ~4,500 feet) 34°07′N 122°30′W (0119 UT to 0200 UT)

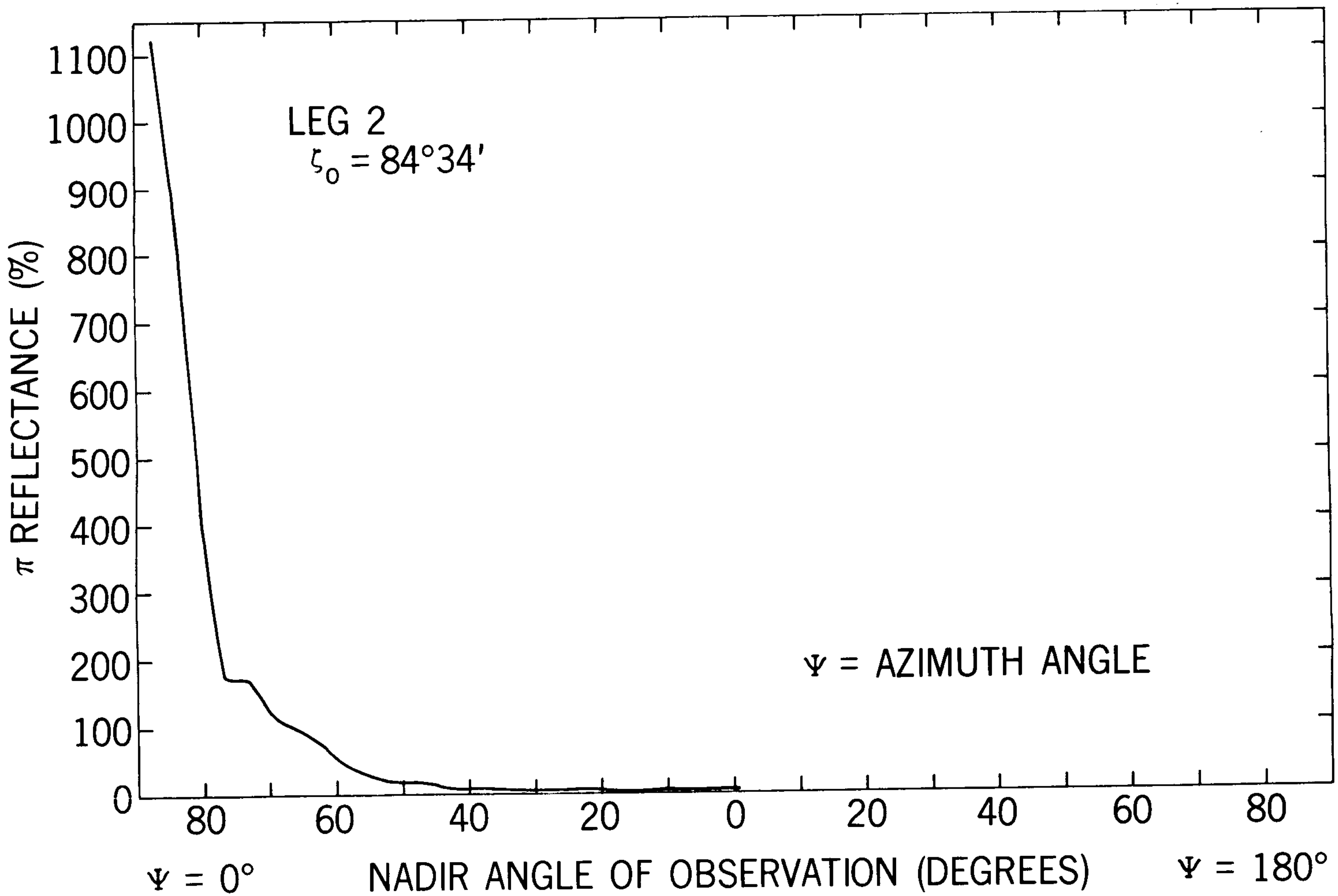

Figure 18. NASA Convair 990 Flight 1, May 6, 1967 (Altitude 29,000 feet) Pacific Ocean, Clear Skies 34°45′N 121°15′W (0211 UT to 0249 UT) MRIR Channel 5 (0.2 to 4μ)

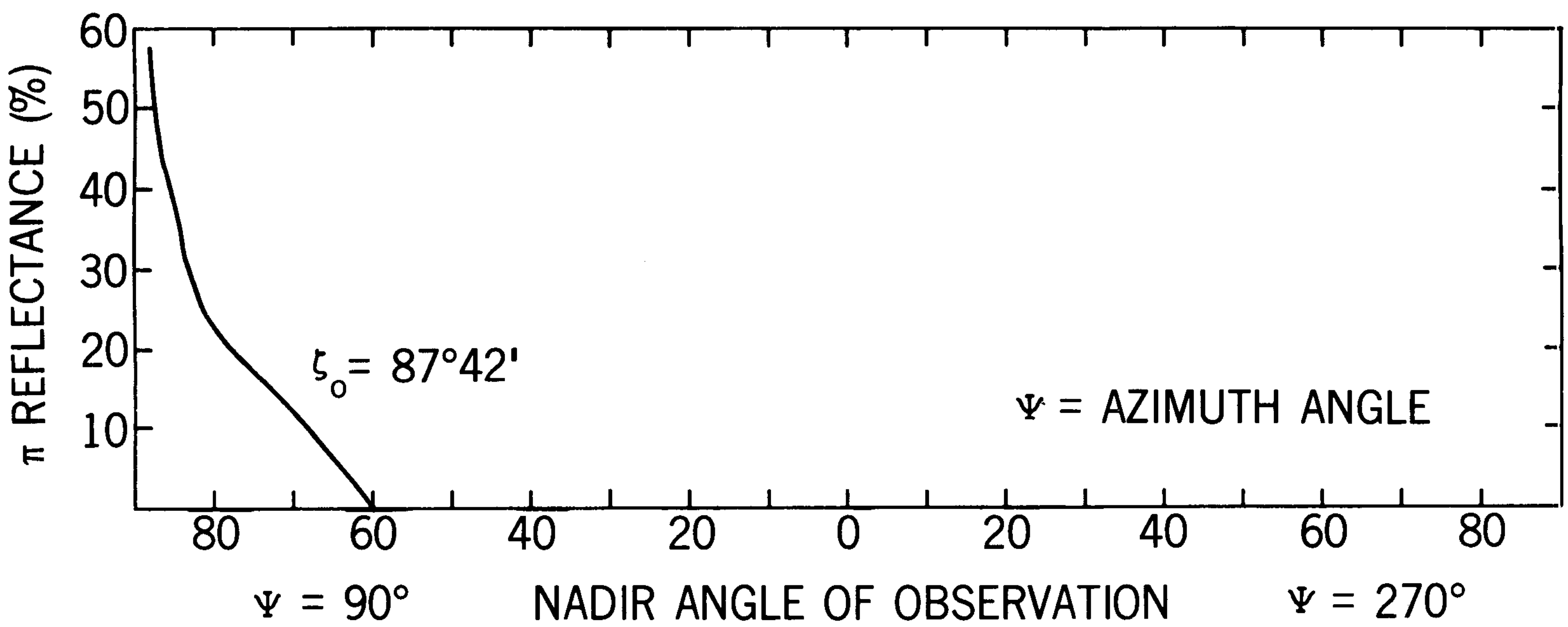

Figure 19. NASA Convair 990 Flight 1, May 6, 1967 (Altitude 29,000 feet) Pacific Ocean, Clear Skies 34°45'N 121°15'W (0211 UT to 0249 UT) MRIR Channel 5 (0.2 to 4μ)

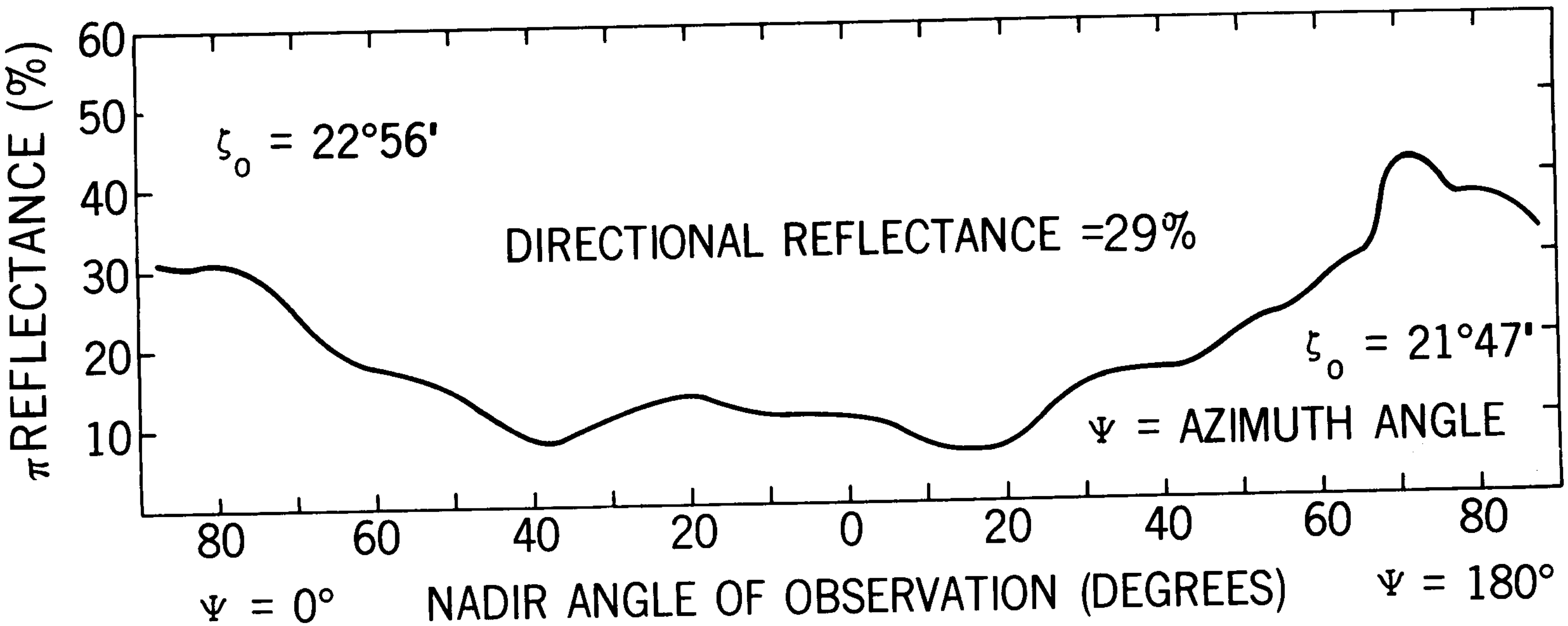

Figure 20. NASA Convair 990 Flight 3, May 9, 1967 (Altitude 25,000 feet) Broken Stratocumulus (Altitude ~ 10,000 feet) 36°48′N 124° 49′W (2100 UT to 2120 UT) MRIR Channel 5 (0.2 to 4μ)

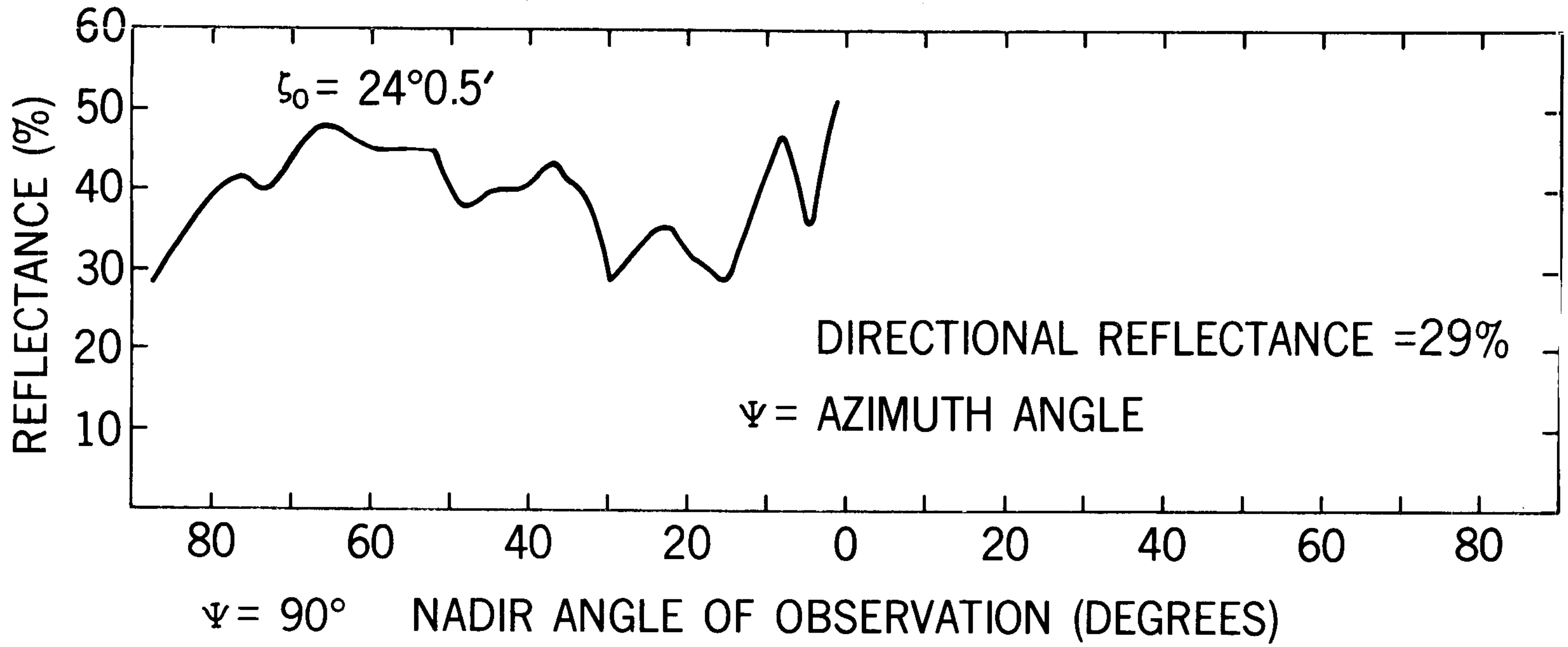

Figure 21. NASA Convair 990 Flight 3, May 9, 1967 (Altitude 25,000 feet) Broken Stratocumulus (Altitude ~ 10,000 feet) 36°48'N 124° 49'W (2100 UT to 2120 UT) MRIR Channel 5 (0.2 to 4μ)

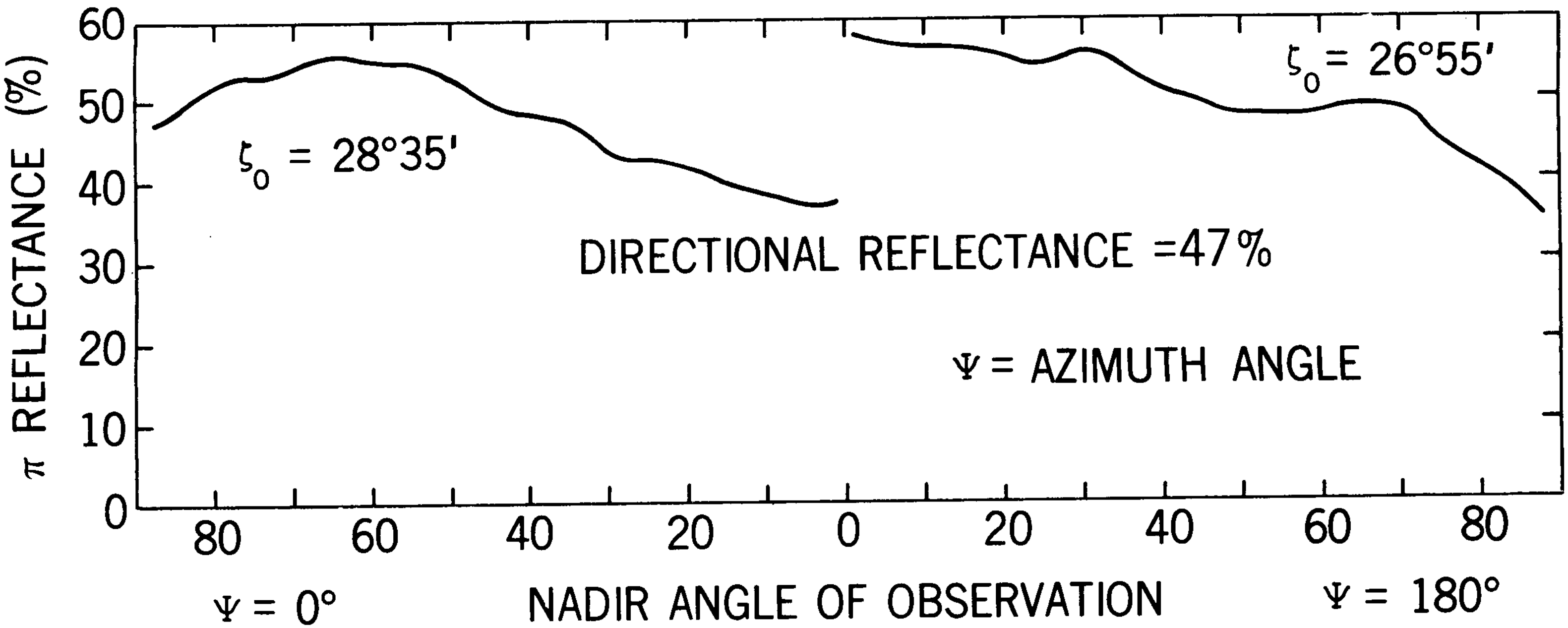

Figure 22. NASA Convair 990 Flight 3, May 9, 1967 (Altitude 35,000 feet) Broken Stratocumulus (Altitude ~ 15,000 feet) 36°48'N 124° 49'W (2135 UT to 2156 UT) MRIR Channel 5 (0.2 to 4μ)

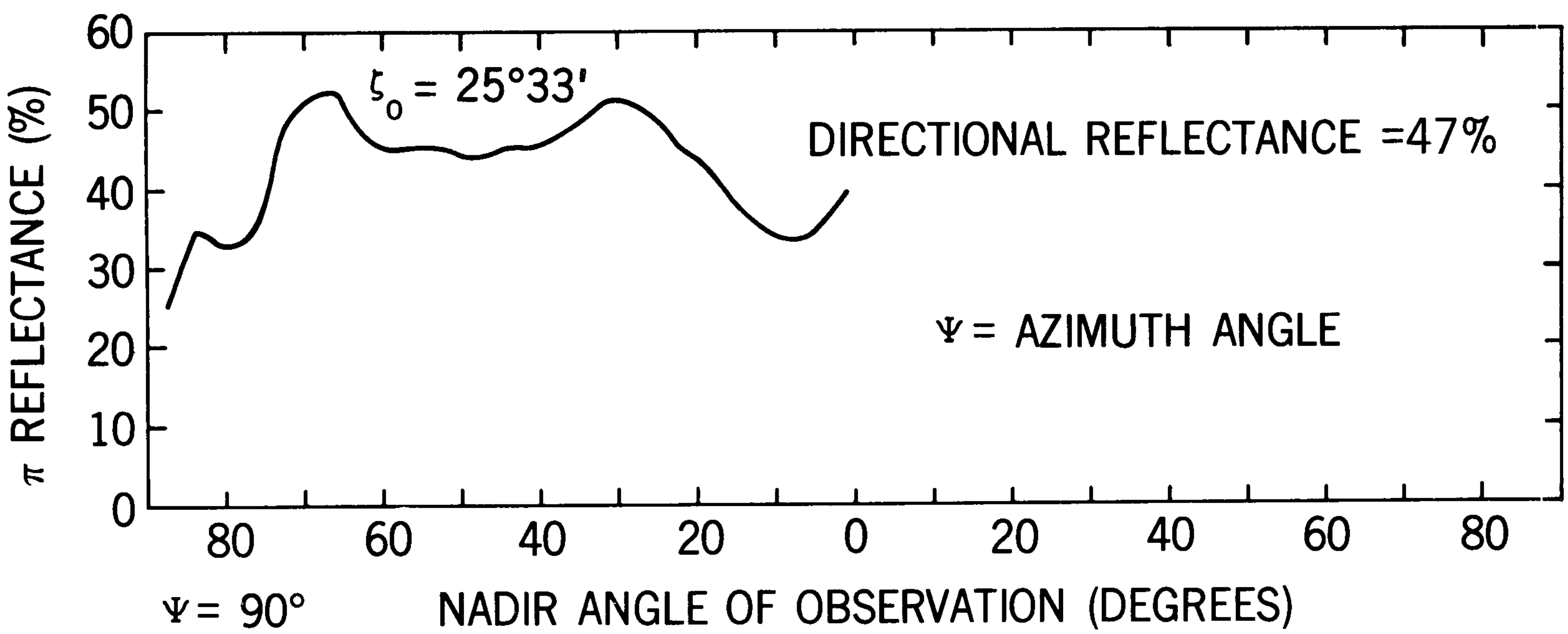

Figure 23. NASA Convair 990 Flight 3, May 9, 1967 (Altitude 35,000 feet) Broken Stratocumulus (Altitude ~ 15,000 feet) 36°48'N 124° 49'W (2135 UT to 2156 UT) MRIR Channel 5 (0.2 to 4μ)

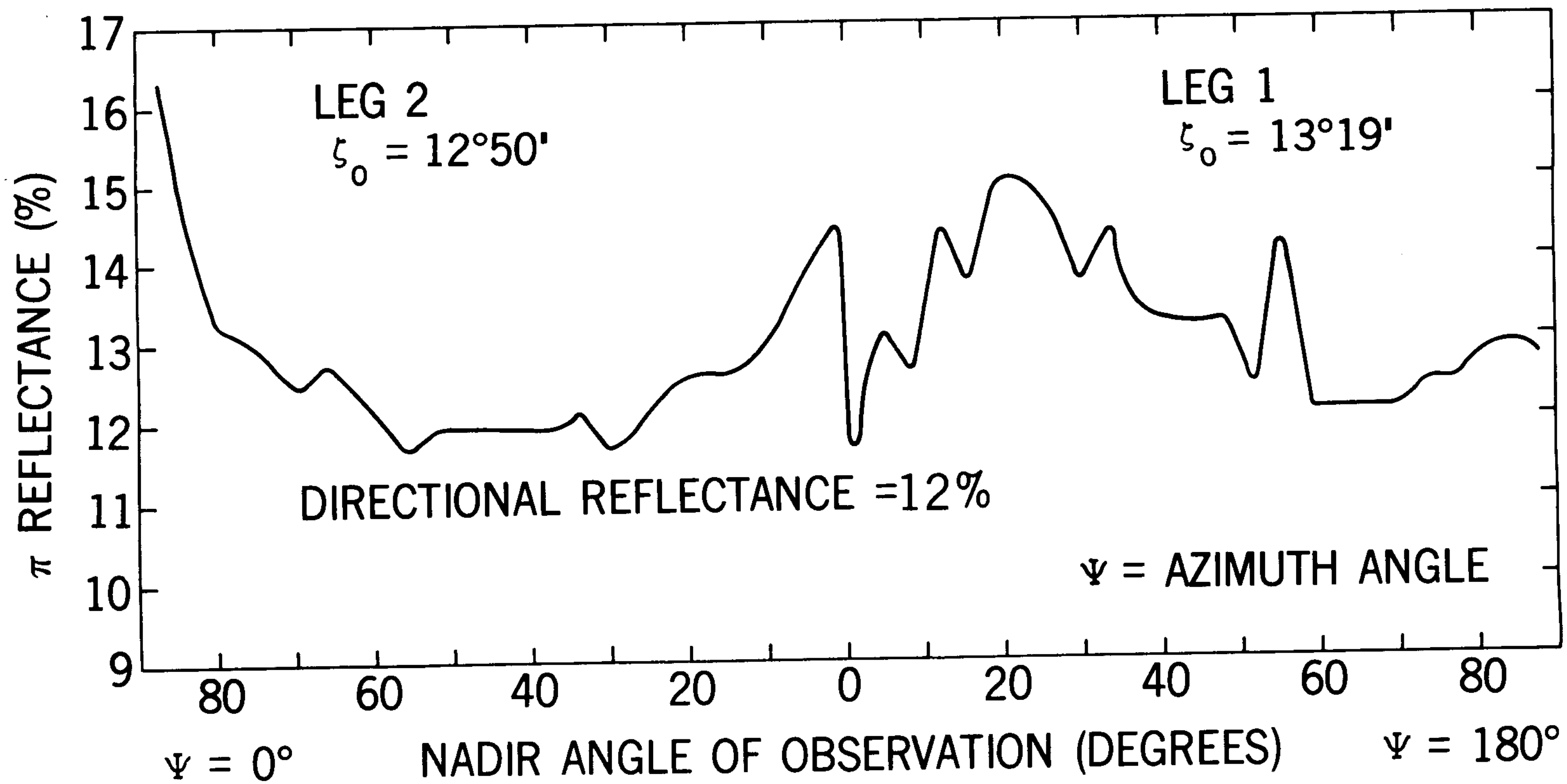

Figure 24. NASA Convair 990 Flight 11, June 3, 1967 (Altitude 33,000 feet) Farmland, Wooded Areas and Patches of Stratus 34°N 95°17'W (1745 UT to 1819 UT) MRIR Channel 5 (0.2 to 4μ)

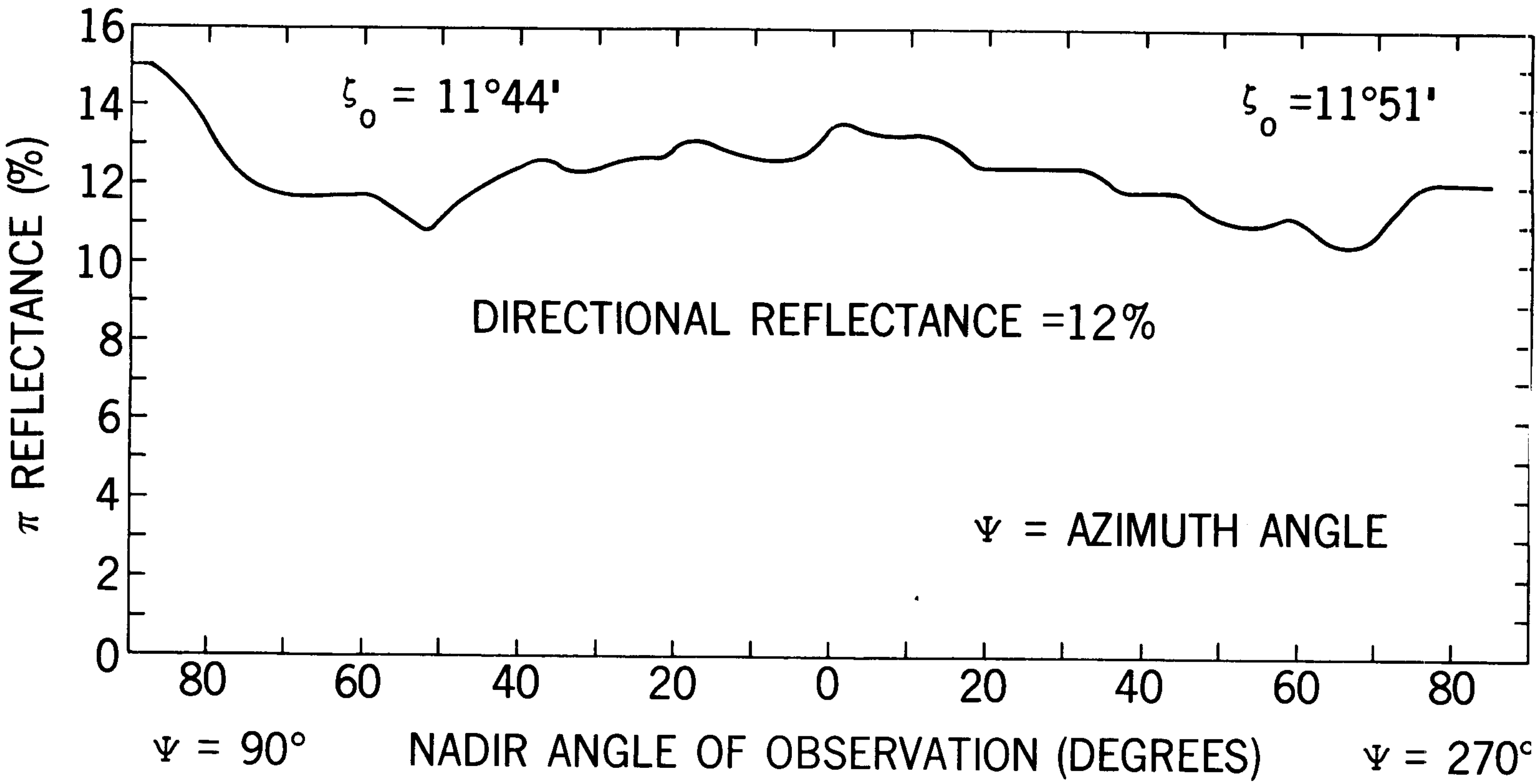

Figure 25. NASA Convair 990 Flight 11, June 3, 1967 (Altitude 33,000 feet) Farmland, Wooded Areas and Patches of Stratus 34°N 95°17'W (1745 UT to 1819 UT) MRIR Channel 5 (0.2 to 4μ)

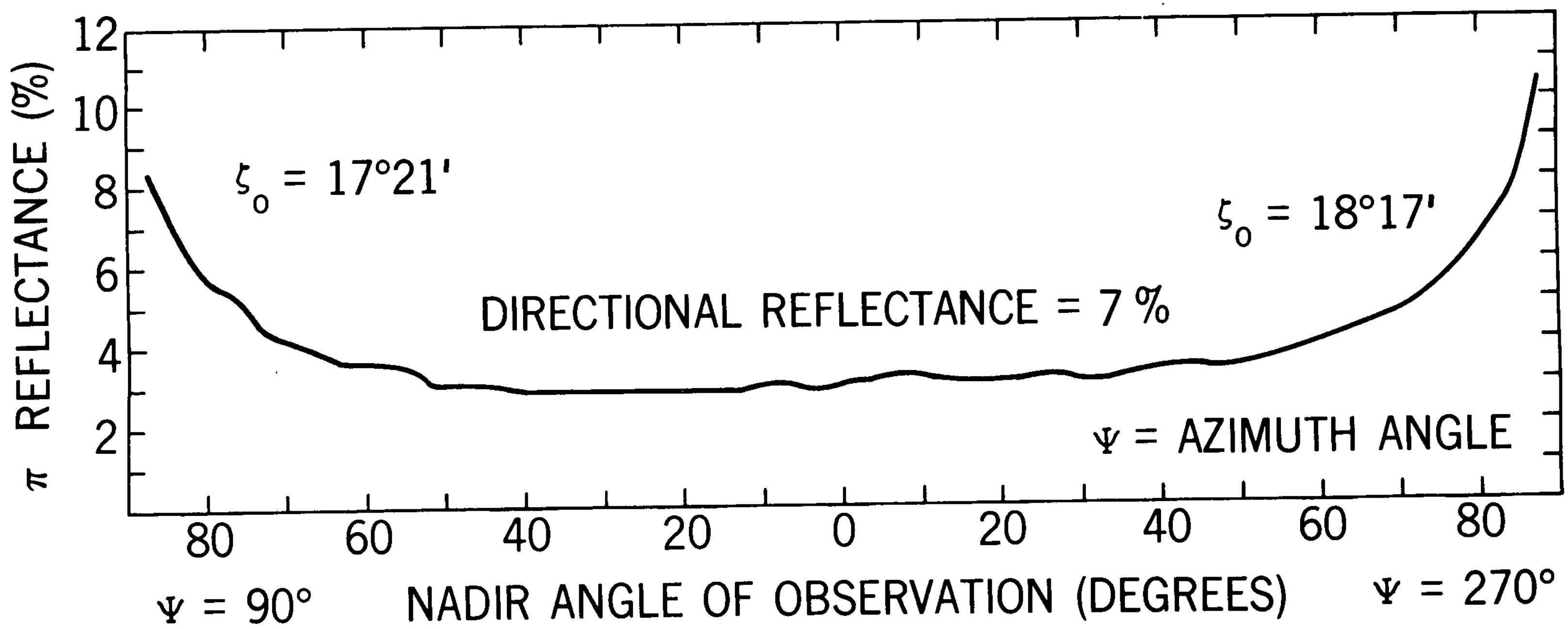

Figure 26. NASA Convair 990 Flight 11, June 3, 1967 (Altitude 38,000 feet) Gulf of Mexico, Clear Skies
29°10'N 93°30'W (2014 UT to 2050UT) MRIR Channel 5 (0.2 to 4μ)

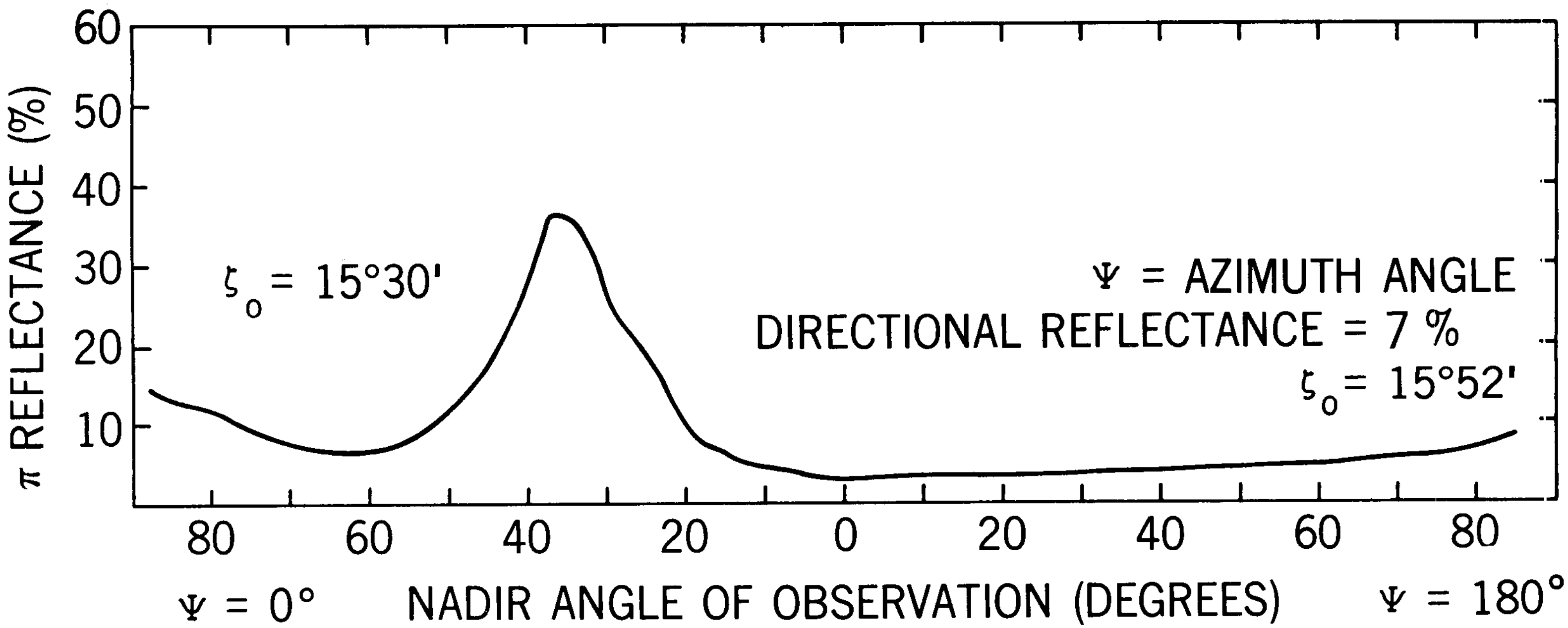

Figure 27. NASA Convair 990 Flight 11, June 3, 1967 (Altitude 38,000 feet) Gulf of Mexico, Clear Skies
29° 10′N 93° 30′W (2014 UT to 2050 UT) MRIR Channel 5 (0.2 to 4μ)